IJET International Journal of Engineering & Technology
CENTRE OF PROFESSIONAL RESEARCH PUBLICATIONS
ISSN 2049-3444
International Journal of Engineering and Technology Volume 6 No.9, September, 2016

Mathematical Modelling of Convective Drying Process of Women's Hair in a Saloon

Onisuru Century Omamoya & Fasogbon Samson Kolawole
Department of Mechanical Engineering, Faculty of Technology, University of Ibadan, Nigeria

ABSTRACT

Drying models are useful in the optimization and control of drying systems to ensure good quality of dried materials. This paper presents a mathematical model for hair drying processes. Specifically, the model is developed for drying processes of women hair in saloons. The modelling is anchored on the conduction-convection heat transfer process, which culminates to the description of the physics of the drying processes; with appropriate boundary conditions being considered. The mathematics of the physics was solved using the method of separation of variable, as it presents itself as the appropriate solution method. The model is able to predict temperature and moisture content distributions of the drying hair; no available experimental data for comparison. However, the trend of results compared well with those of particular case of lump models. Simulations based on this model were conducted to study the effects of operational parameters (namely, air temperature, heat and mass transfer coefficients and thermal diffusivities) on the moisture content and temperature of the hair. Simulation results show that increasing the air temperature and velocity decrease drying rate. It is evident from the simulations that sample with high thermal diffusivity and coefficient of diffusion values exhibits shorter duration of drying.

Keywords: *Analytical Solution, Convective Drying Process, Heat and Mass Transfer, Mathematical Modelling, Porous Media.*

1. INTRODUCTION

Drying is a heat and mass transfer process, which involves removing moisture by evaporation. It is the removal of moisture from a wet product by thermal process. The objective of drying is to produce a dried product of desired quality (Mujumdar, 2007), to enhance the quality and life span of these products and also to facilitate their storage and transportation (Jamaleddine and Ray, 2010). Drying is an essential operation in the Chemical, Agricultural, Biotechnology, Food, Polymer, Ceramics, Pharmaceutical, Pulp and Paper, Mineral and Wood processing industries (Mujumdar, 2004).

In general, drying is accomplished by thermal techniques and thus involves the application of heat, most commonly by conduction and convection processes. Throughout the convective drying of solid materials, two process occur simultaneously namely; transfer of energy from the local environment in the dryer and transfer of moisture from within the solid; this unit operation is considered as simultaneous heat and mass transfer operation. In drying, wet materials loses moisture in direct contact with hot air. The hot air supplies the energy required for drying and also carries away the moisture released by the solid (Basirati and Hamdullahpur, 2007).

Hair drying is a routine operation job carry-out by hair stylish globally. Many appliances used for hair drying are normally produced in the Western world, and imported to Africa nations. The design parameters are normally based on the morphology of Western world human hairs. There is a great distinct between the Western human hair and those of the sub-Sahara African, which may render the functionality of imported hair drier not been optima. The drying of hair, especially the convective drying process of women's hair in a saloon, is characterized by a high level of initial moisture after washing. Optimum drying of human hairs has an important role in final hair texture, homogeneity and flexibility. It is, therefore, required on general note to design dryers that are based on sub-Sahara Africa women's parameters. Hair drying in the saloon has become an important industrial development worldwide similar to other technologically advanced process industries. Widespread methods of hair drying all over the world are mostly force convectional and required a lot of energy.

Currently, most dehydrated hairs are produced by the technique of hot air drying, which is the simplest and most economical of the various methods (Crank, 1975). However, for modelling purposes, in this study, force convectional hot air drying is assumed to be applied to the surface. The main feature of such system is its ability to predict moisture and temperature inside the product. The objective of this present work is, therefore, to develop mathematical models which could capture the basic physics during convection drying of sub-Sahara Africa women's hairs.

2. MATERIAL AND METHOD

A rectangular portion of woman's hair of 500mm in length and 200mm in thickness is considered, as depicted by Figure. 1. The rectangular portion of the hair is considered to be soaked with water and entrained air bubbles; the material is considered a porous material. Although the thickness is small, however, the process could not be modelled as lumped parameter, as the time considered for the drying process does not permit for large time scale. It is expected that temperature and moisture both vary in time and depth (from the drier side to the scalp). The methodology is on analytical solution anchored on separation of variable, as the appropriate solution method to the field problem.

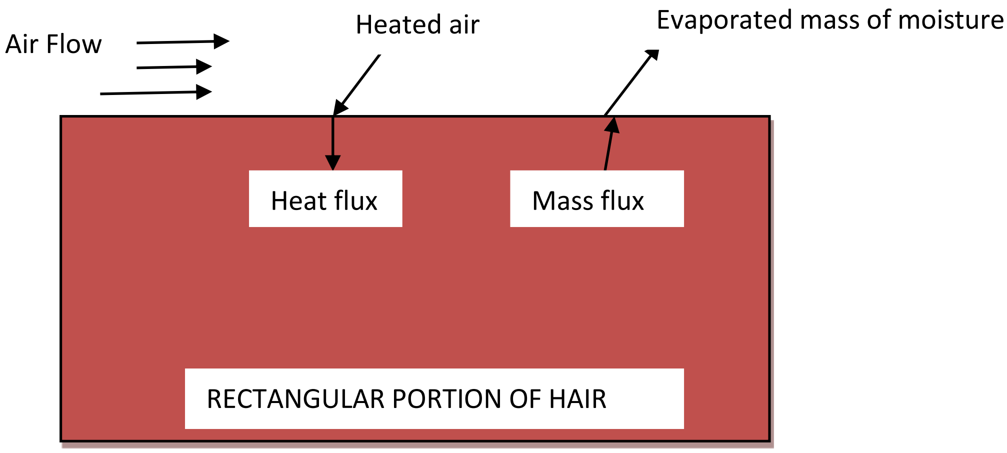

Figure 1: Schematic diagram of heat and mass transfer during drying of hairs

Figure 2 shows the simplified 2D axisymmetric geometry used for modeling. Due to axial symmetry only one quarter of a planer intersection was considered for simulation.

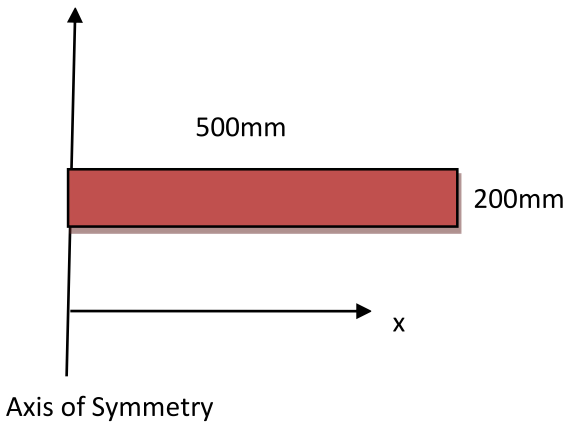

Figure 2: Simplified 2D axisymmetric model

2.1. Model Development

These assumptions were made in the process of developing the models:

- One dimensional heat and mass transfer
- Uniform initial temperature and moisture distribution
- Negligible shrinkage during drying
- Constant physical properties of hair
- The material is considered homogeneous and isotropic
- The origin of the axis x is located at the central point of the material i.e 2D axisymmetric geometry.

This transport process of heat experiences an increases in hair temperature towards air temperature due to inwards flux of heat and a decrease in temperature due to outward heat flux because of evaporation (Barati and Esfahani, 2011).The governing physical equations for simultaneous transfer of moisture M (x,t) and temperature, T(x,t) in an isotropic rectangular portion of hair is given by the coupled parabolic partial differential equations (Luikov, 1968; crank, 1992).

$$\frac{\partial M}{\partial t} = D\frac{\partial^2 M}{\partial X^2} \qquad (1)$$

$$\rho C_P\frac{\partial T}{\partial t} = K\frac{\partial^2 T}{\partial X^2} \qquad (2)$$

Where D is diffusion coefficient, ρ is density, C_p is specific heat and k is thermal conductivity.

The effective mass diffusivity as a function of drying air temperature can be determined by Arrhenius type equation (Nastaj and Witkiewicz, 2009) as:

$$D_{eff} = D_o \exp\left(\frac{-E_a}{R(T_{air}+273.15)}\right) \quad (3)$$

In equation (3), D_o is a pre-exponential factor (M^2 S^{-1}), Ea is the activation energy (J.mol-1) and R is the universal gas constant (8.314 J.mol^{-1} k^{-1}).

Average heat transfer coefficient was calculated from the following equation (Mills 1995) for laminar and turbulent flow respectively:

$$Nu = \frac{h_T L}{k} = 0.664 Re^{0.5} Pr^{0.33} \quad (4)$$

$$Nu = \frac{h_T L}{k} = 0.0296 Re^{0.5} Pr^{0.33} \quad (5)$$

As Fourier's law and Fick's law are identical in mathematical form, the analogy is used to find mass transfer coefficient. Nusselt number and Prandtl number are replaced by Sherwood number and Schmidt number respectively in the following relationship:

$$Sh = \frac{h_m L}{k} = 0.332 Re^{0.5} Sc^{0.33} \quad (6)$$

$$Sh = \frac{h_m L}{k} = 0.0296\, Re^{0.5} Sc^{0.33} \quad (7)$$

Where, $Re = \frac{\rho_a V l}{\mu_a}, Sc = \frac{\mu_a}{\rho_a D}\, and\ \mathrm{Pr} = \frac{C_p \mu_a}{K_a}$

2.2. Mathematical Analysis:

2.2.1. Mass Transfer

$$\frac{\partial M}{\partial t} = D\frac{\partial^2 M}{\partial x^2};\ \text{in } 0 < x < L \quad (8)$$

Subject to the following boundary and initial conditions:

$$\frac{\partial M}{\partial x} = 0;\ \text{at} M(0,t) \quad (9a)$$

$$D\frac{\partial M}{\partial x} = -h_m(M - M_{air});\ \text{at} M(L,t) \quad (9b)$$

$$M = M_i\ ;\ \text{at} M(x,0) \quad (9c)$$

These mass transfer equations suggest that the transport of moisture through the material is as a result of the influence of concentration gradient within the moist material.

Taking $\vartheta \equiv M - M_{air}$, eq. (8) and (9) could be written as:

$$\frac{\partial \vartheta}{\partial t} = D\frac{\partial^2 \vartheta}{\partial x^2};\ \text{in } 0 < x < L \quad (10)$$

Subject to the following boundary and initial conditions:

$$\frac{\partial \vartheta}{\partial x} = 0;\ \text{at}\vartheta(0,t) \quad (11a)$$

$$D\frac{\partial \vartheta}{\partial x} = -h_m \vartheta;\ \text{at}\vartheta(L,t) \quad (11b)$$

$$\vartheta = \vartheta_i\ ;\ \text{at}\vartheta(x,0) \quad (11c)$$

To solve this problem, one assumes the separation of function $\vartheta(x,t)$ into space- and time-dependent functions (Jiji, 2009) in the form of;

$$\vartheta(x,t) = \eta(x)\Omega(t) \quad (12)$$

The substitution of eq. (12) into (10) gives:

$$\frac{1}{\eta(x)}\frac{d^2\eta(x)}{dx^2} = \frac{1}{D\Omega(t)}\frac{d\Omega(t)}{dt} \quad (13)$$

Eq. (13) holds when both sides are equal to the same constant, say $-\beta^2$, hence, one obtains;

$$\frac{1}{\eta(x)}\frac{d^2\eta(x)}{dx^2} = \frac{1}{D\Omega(t)}\frac{d\Omega(t)}{dt} = -\beta^2 \quad (14)$$

This implies that the function $\Omega(t)$ satisfies the differential equation

$$\frac{d\Omega(t)}{dt} + D\beta^2\Omega(t) = 0 \quad (15)$$

This has a general solution in form of

$$\Omega(t) = e^{-D\beta_m^2 t} \quad (16)$$

The space-variable function $\eta(x)$ satisfies the differential equation (Faghri et al, 2010)

$$\frac{d^2\eta(x)}{dx^2} + \beta^2\eta(x) = 0 \quad (17)$$

Equation (17) holds according to (Ozisik, 1993):

$$\beta_m tan\beta_m L = \frac{h_m}{D} \quad (18)$$

The mass transfer equation is, thus;

$$\vartheta(x,t) =$$

$$2\sum_{m=1}^{\infty}\left[\frac{\beta_m^2 + \left(\frac{h_m}{D}\right)^2}{L\left\{\beta_m^2 + \left(\frac{h_m}{D}\right)^2\right\} + \frac{h_m}{D}}(\cos\beta_m x)e^{-D\beta_m^2 t}\frac{\vartheta_i}{\beta_m}(\sin\beta_m L)\right]$$

(19)

Where, β_m are the positive roots of eq. (18)

2.2.2. Heat Transfer

$$\frac{\partial T}{\partial t} = \alpha \frac{\partial^2 T}{\partial x^2}; \text{ in } 0 < x < L \quad (20)$$

Subject to the following boundary and initial conditions:

$$\frac{\partial T}{\partial x} = 0; \text{ at} T(0,t) \quad (21a)$$

$$k\frac{\partial T}{\partial x} = -h(T - T_{air}) + L_w h_m (M - M_{air}); @\ T(L,t) \quad (21b)$$

$$T = T_i\ ; \text{ at} T(x,0) \quad (21c)$$

Taking $\theta \equiv T - T_{air}$, eq. (20) and (21) are transformed to become:

$$\frac{\partial \theta}{\partial t} = \alpha \frac{\partial^2 \theta}{\partial x^2}\ ; \text{ in } 0 < x < L \quad (22)$$

Subject to the following boundary and initial conditions:

$$\frac{\partial \theta}{\partial x} = 0; \text{ at} \theta(0,t) \quad (23a)$$

$$k\frac{\partial \theta}{\partial x} = -h\theta + L_w h_m \vartheta; @\ \theta(L,t) \quad (23b)$$

$$\theta = \theta_i\ ; \text{ at} T(x,0) \quad (23c)$$

Separation of variable is applied to eq. (22), thus (Jiji, 2009):

$$\theta(x,t) = \varphi(x)\Gamma(t) \quad (24)$$

Substituting eq. (24) into (22) gives

$$\frac{1}{\varphi(x)}\frac{d^2\varphi(x)}{dx^2} = \frac{1}{\alpha\Gamma(t)}\frac{d\Gamma(t)}{dt} \quad (25)$$

This can be separated by introducing a separation constant as:

$$\frac{1}{\varphi(x)}\frac{d^2\varphi(x)}{dx^2} = \frac{1}{\alpha\Gamma(t)}\frac{d\Gamma(t)}{dt} = -\lambda^2 \quad (26)$$

Therefore,

$$\frac{d\Gamma(t)}{dt} + \lambda^2\alpha\Gamma(t) = 0 \quad (27)$$

While,

$$\frac{d^2\varphi(x)}{dx^2} + \lambda^2\varphi(x) = 0 \quad (28)$$

Following through the method adopted in the mass transfer analysis, one obtains:

$$\Gamma(t) = e^{-\alpha\lambda_n^2 t} \quad (29)$$

The space-variable function $\eta(x)$ satisfies the differential equation

$$\frac{d^2\varphi(x)}{dx^2} + \lambda^2\varphi(x) = 0 \quad (30)$$

The general solution of eq. (30) is

$$\varphi(x) = G_n\, \varphi(\lambda_n, x) + J_n \varphi(\lambda_n, x) \quad (31)$$

Hence,

$$\tan\lambda_n L = \frac{\lambda_n\left(\frac{h}{k} + \frac{L_w h_m}{k}\right)}{\lambda_n^2 - \frac{h L_w h_m}{k^2}} \quad (32)$$

Considering eq. (32),

One obtains the heat transfer equation as:

$$\theta(x,t) = 2\sum_{n=1}^{\infty}\left\{\left[\left\{\lambda_n^2 + \left(\frac{h}{k}\right)^2\right\}\left(L + \frac{\left(\frac{L_w h_m}{k}\right)}{\lambda_n^2 + \left(\frac{L_w h_m}{k}\right)^2}\right) + \frac{h}{k}\right]^{-1} \left(\lambda_n \cos\lambda_n x + \left(\frac{h}{k}\right)\sin\lambda_n x\right)\theta_i \left[\sin\lambda_n x - \left(\frac{h}{\lambda_n k}\right)\cos\lambda_n x + \left(\frac{h}{\lambda_n k}\right)\right] e^{-\alpha\lambda_n^2 t}\right\} \quad (33)$$

The eigenvalues λ_n are the positive roots of eq. (3

3. RESULTS AND DISCUSSION

The input data for the current analysis are presented in Tables 1 and 2.

Table 1: Input Properties of hair, water and air at 6^0C

Parameters & Symbols	Values	Sources
Density of hair, $\boldsymbol{\rho_{hair}}$	1,100kg/m^3	
Thermal conductivity of hair, $\boldsymbol{K_{hair}}$	0.25 W/m.k	(Guoqing et al, 2014)
Specific heat of hair, $\boldsymbol{Cp_{hair}}$	1.602 KJ/kg.K	
Thermal diffusivity of hair, $\boldsymbol{\alpha_{hair}}$	1.42x10^{-7} m^2/s	(Worthmann et al, 2010)
Activation energy for hair, Ea_{hair}	263kJ/mol	(Zhang et al, 2011)
Diffusion coefficient of hair, $\boldsymbol{D_{eff}}$	1.60x10^{-10} m^2/s	
Initial moisture content of hair, $\boldsymbol{M_o}$	6.4kg/kg db	
Mass transfer coefficient, $\boldsymbol{h_m}$	4.6161x10-9 m^2/s	
Length of hair, $\boldsymbol{L}$	0.2m	
Density of water, $\boldsymbol{\rho_w}$	1000 kg/ m^3	
Latent heat of Evaporation, $\boldsymbol{L_w}$	2358600J/kg	
Specific heat of water, $\boldsymbol{Cp_w}$	4184 J/kg k	
Absolute Viscosity of water, $\boldsymbol{\mu_w}$	0.467x 10^{-3}Pa.s	
Kinematic Viscosity of water, $\surd_w$	0.475x10^{-6}m^2/s	(Kumar et al 2012)
Density of air, $\boldsymbol{\rho_{air}}$	1.073kg/m^3	
Thermal conductivity of air, K_{air}	0.0287 W/m.K	(Mills, 1995)
Dynamic Viscosity of air, $\boldsymbol{\mu_{air}}$	1.78x10^{-4}Pa.s	
Specific heat of air, $\boldsymbol{Cp_{air}}$	1005.04 J/kg.K	(Datta, 2007)
Heat transfer Coefficient of air, $\boldsymbol{h_T}$	2.572 W/m^2.K	
Initial temperature of air, $\boldsymbol{T_0}$	25^{0}C	
Relative humidity of air, R.H	31.29%	(Clarence, 2012)

Table 2: Values of Dimensionless numbers and Transfer Coefficients

S/no	Quantity	Symbol	Unit	Formula & value
1.	Reynolds Number	Re_{air}	---	$\frac{\rho_{air}VL}{\mu_{air}} = 964.493$
2.	Prandtl Number	Pr	---	$\frac{C_p\mu_{air}}{K_{air}} = 0.654$
3.	Nusselt Number	Nu	---	$0.664\ R_e{}^{0.5}P_r{}^{0.33} = 17.925$
4.	Heat Transfer Coefficient	h_T	$W/m^2.K$	$h_T = N_u * K_{air}/L = 2.572$
5.	Schmidt Number.	S_c	---	$\surd_{hair}/D_{eff} = 2968.75$
6.	Sherwood Number	Sh	---	$0.332R_e{}^{0.5}S_c{}^{0.33} = 144.29$
7.	Mass Transfer Coefficient	h_m	m^2/s	$h_m = Sh * D_{eff}/L = 4.6161\ 10^{-9}$

The results of simulations of the developed mathematical models executed with integrated programming environment are here presented;

Figure 3 shows the simulation of moisture content with variation of temperature. It can be inferred from the figure that increasing the temperature of the hair increases the relative humidity of the hot air which is attributed to water evaporation from the drying hair to the drying medium (the hot air). If such hot air is in contact with a wet hair, the rate of moisture migration from the hair to the hot air through evaporation will be increased, which is the mechanism behind the hair drying process. Therefore, at high temperatures the moisture content of the hair reduces, whereas at low temperatures the moisture content of the hair increases. This is due to the fact that the moisture diffusivity increases with the increase in temperatures thereby resulting in a decrease in the amount of moisture in the hair and also that the relative humidity of water decreases with increase in temperature. The deficit in relative humidity of drying medium is a strong driving force in drying processes (concentration gradient). This observation from the simulation is in good agreement with trends presented in the literatures (Methakhup et al, 2004; Prabhanjan et al, 1995).

.

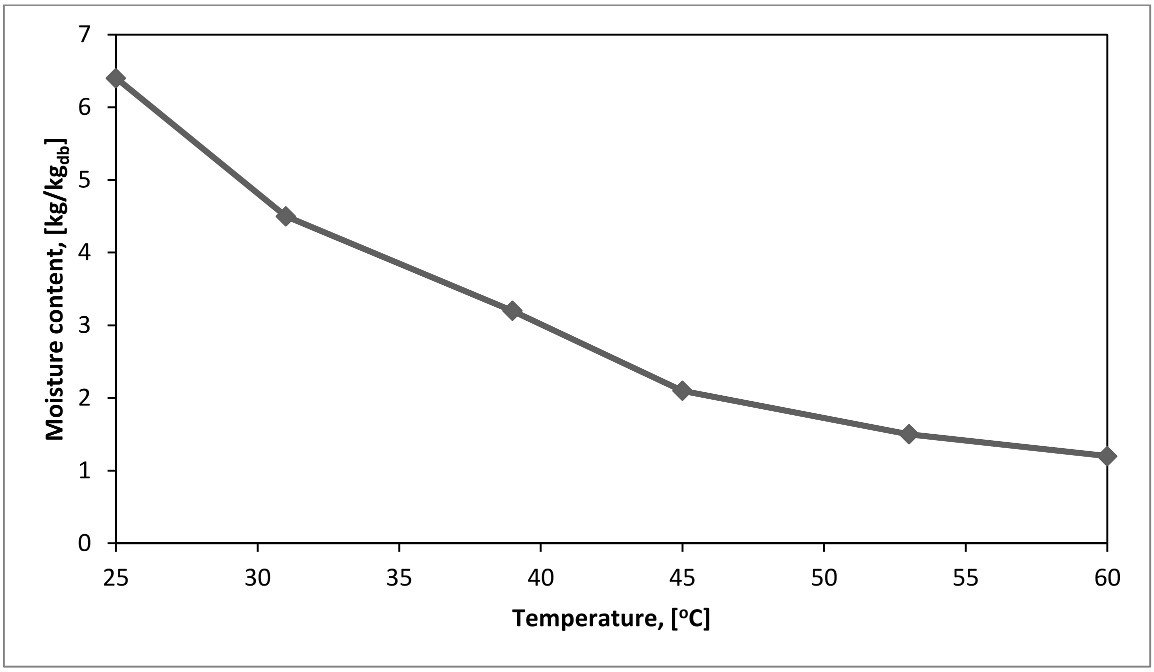

Figure 3: Profile of moisture content against temperature

Figure 4 shows moisture distribution with the drying time. The curve represents the gradient of moisture at different drying times. It shows that as drying time increases, the moisture content at each location of the hair decreases until the equilibrium moisture content is reached, which is confirmed by experimental findings presented in (Quiroz, 2001; Simal et al, 2005). This trend could be used to control the hair drying process, which is a major parameter in driers.

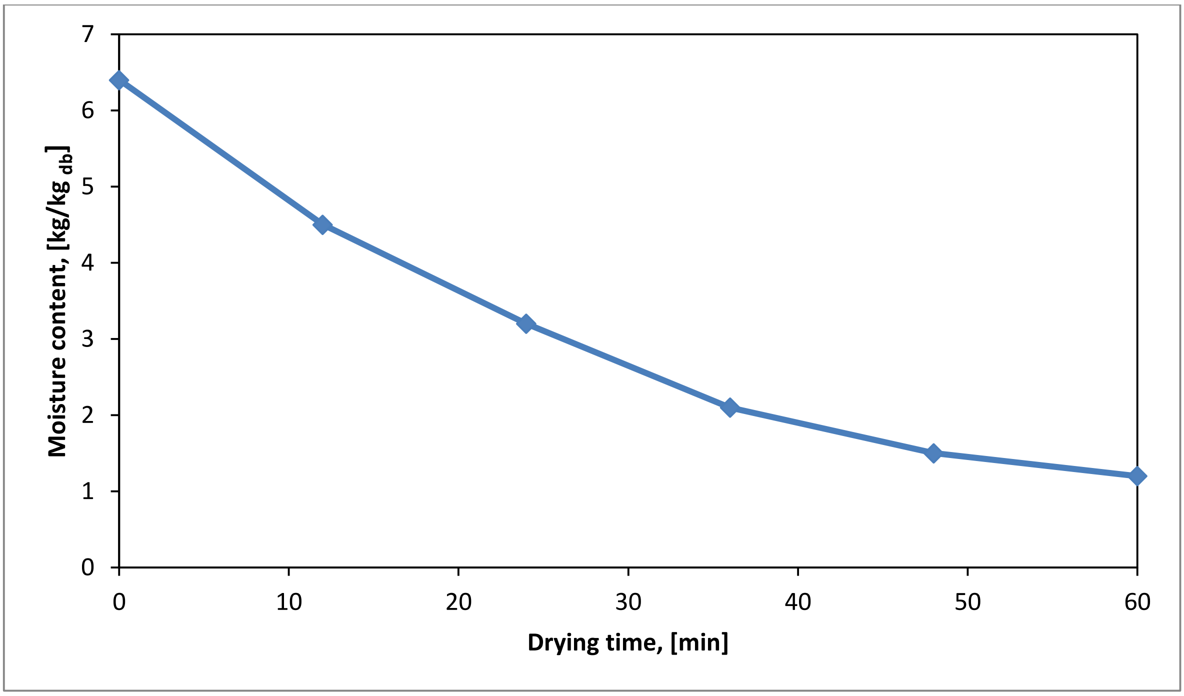

Figure 4: Variation of moisture content with drying time

It is clear from Figure 5 that the hair temperature increases at the initial stage up to the saturation temperature, at which point, evaporation of moisture from the hair starts. From that point, the hair temperature increases with drying time as a result of the difference between the moisture contents at the surface and the centre of the hair. This is the beginning of the falling rate period and the hair starts to dry from the surface while the moisture in the interior is being transferred to the surface for evaporation. This observation is clearly demonstrated by the simulated results in Figure 5. The increases in the air temperature over time also increase the material temperature of the hair, hence fast drift of moisture towards the surface of the hair for evaporation. It also illustrates that increase in the material temperature results in a rise in the drying time which conforms to available literatures (Kumar, 2012; Haghi and Rondot, 2004).

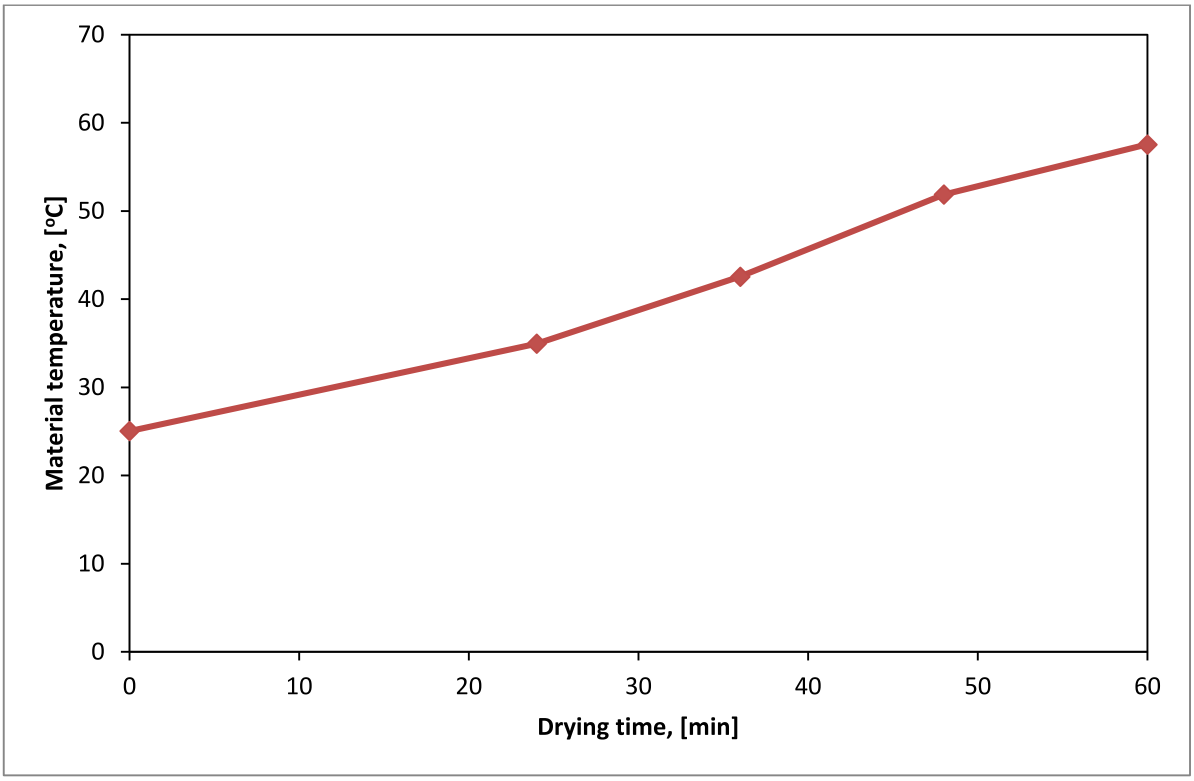

Figure 5: Material temperature versus drying time

It can be seen form Figure 6 that drying rate is not constant throughout the drying period. The drying rate reduces monotonously with reduction in moisture content of the hair. The initial drying rate decreased from 0.0035 to 0.024 while moisture content decreases from 0.2082 to 0.1421. This observation implies that drying rates of hair are majorly dependent on temperature in which the hair is exposed. In drying, it is expected that the water that is loosely held will be removed most easily. The drying rate being the amount of evaporated moisture content over time, it is clear that the drying rate is highest during the initial period of the drying and often decreases gradually. The moisture content of the hair was equally very high at the initial phase of drying which resulted in higher drying rates due to higher moisture diffusion. As the drying progresses, the loss of moisture content in the hair resulted in a decrease in the drying rates. Thus it would be expected that drying rates would decrease as moisture content decreases, with the remaining water being bound more and more strongly as its quantity decreases. No evidence of constant drying curve period can be found in the drying curve presented for hair, as demonstrated in Figure 6. This observation is in agreement with

previous studies (Ayensu, 2003, 2004; Davishi et al, 2013; Evin, 2011; Afolabi and Agarry, 2014).

.

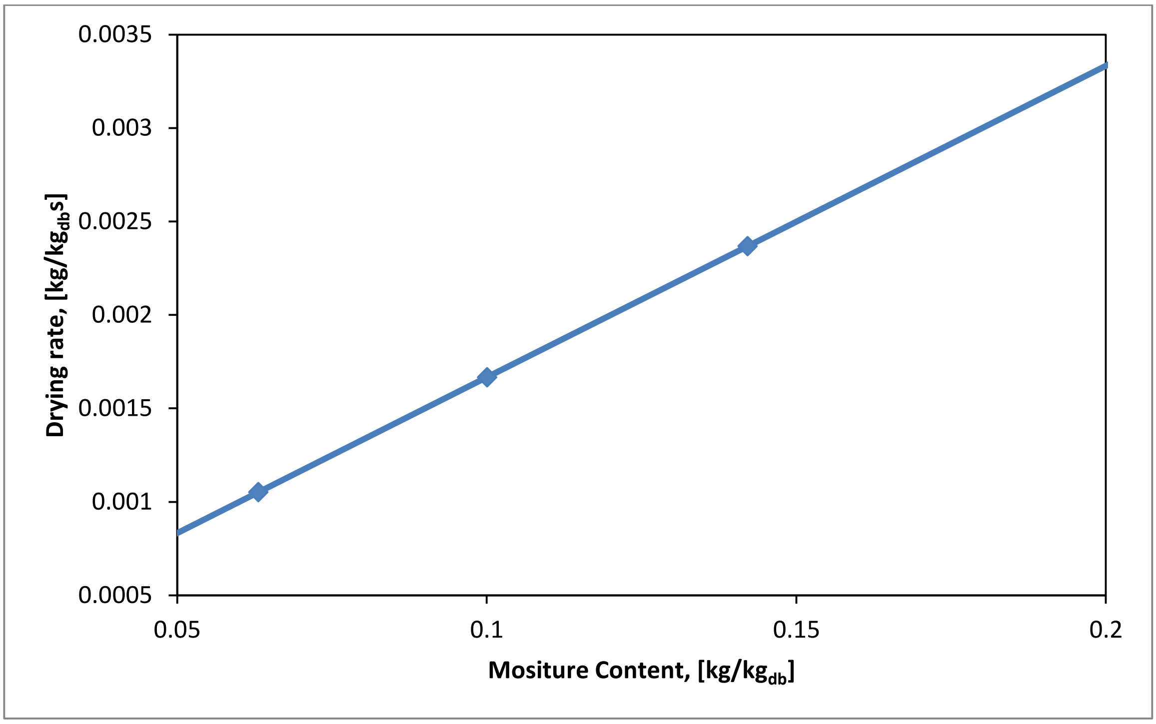

Figure 6: Drying rate and moisture content profiles for air temperature of 50 ^{0}C and velocity of 0.8m/s

Table 3: Simulation Results

X (m)	t(min)	$\theta(^0C)$	$\vartheta(kg/kg\ db)$
0.00	0.00	25.00	6.40
0.40	12	34.95	0.208
0.80	24	42.56	0.202
0.12	36	51.86	0.200
0.16	48	57.55	0.192

From Table 3 above, the simulation results shown that the model was able to predict the temperatures and moisture contents of the hair with respect to time during drying at different points along the length of the hair. At the base of the hair 0.00m and at time 0.00min, the initial moisture content and temperature were 6.40kg/kg db and 25^{0}C. As drying continues, and at a distance 0.40m from the base of the hair and at time 12minutes, the temperature of the hair rose to 34.95^{0}C while the moisture content reduced to 0.208kg/kg db. Further drying of the hair increases the temperature from 34.95^{0}C to 42.56^{0}C and the moisture content reduces from 0.208kg/kg db to 0.202kg/kg db at time 24minutes and 0.80m distance. When the time of drying reaches 36minutes, temperature rises to 51.86^{0}C while moisture content drops to 0.200kg/kg db at 0.12m distance from the hair scalp. Finally, at the tip of the hair where you have the highest simulation temperature of 57.55^{0}C, the hair was completely dried up to 0.192kg/kg db moisture content when the dryer has worked for 48minutes. This further elaborates the efficiency of the developed models and conforms to the figures and literatures earlier cited.

3.1. Model Validation

The model was validated with a Dyson Supersonic™ hair dryer of rated power 1600W. The input energies of both the model and Dyson Supersonic™ hair dryer were calculated and programmed with matlab computer language. The results were compared and examined.

Figure 7 Dyson supersonic™ hair dryer, 212⁰F- Fast drying and styling, 176⁰F-Regular drying, 140⁰F- Gentle drying

3.1.1. Energy Utilized

The amount of energy utilized is computed using the formula (Srisittipokakun et al, 2012)

$$\text{Energy utilized (J/s)} = {}^{M_w L_w}/_{t} \qquad (34)$$

Where M_w = Mass of water evaporated (kg), L_w = Latent heat of vaporization of water (kJ/kg) and t= time (second).

3.1.2. Efficiency of Hair Dryer

The dryer efficiency can be calculated from the relation:

$$\eta = \frac{{}^{M_w L_w}/_{t}}{\text{power input}} \qquad (35)$$

The power input of the Dyson supersonic™ hair dryer is 1600W while the estimate average efficiency of the model is 70%.

Figure 7 shows the amount of energy utilized by Dyson supersonic™ hair dryer and the developed model. It showed that energy utilized by Dyson supersonic™ hair dryer is higher as compared to the model; it implies that the higher amount of energy used by Dyson supersonic™ hair dryer leads to faster drying rate and higher efficiency (100%). The model was able to conserve energy and efficient in its task within the stipulated time.

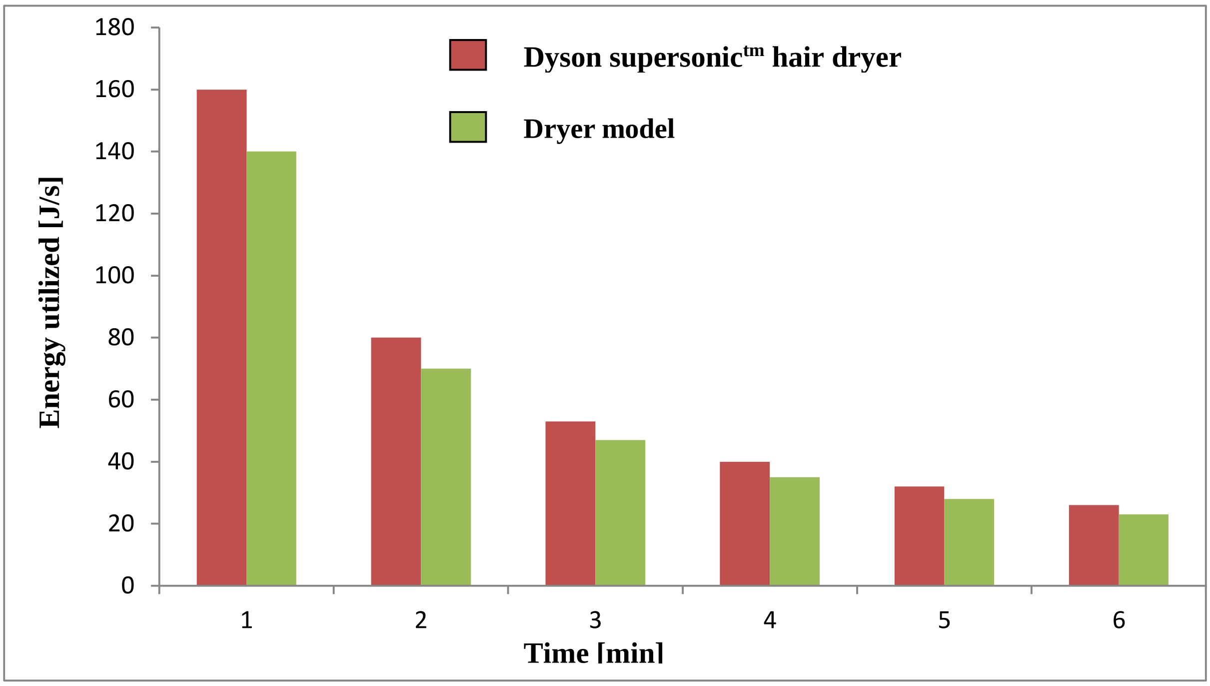

Figure 8: Energy utilized in Dyson supersonic^{TM} hair dryer and Model

4. CONCLUSION

Hair drying is a routine operation job carry-out by hair stylish globally. Many appliances used for hair drying are normally produced in the Western world, and imported to Africa nations. The design parameters are normally based on the morphology of Western world human hairs. There is a great distinct between the Western human hair and those of the sub-Sahara African, which may render the functionality of imported hair drier not been optima. The drying of hair, especially the convective drying process of women's hair in a saloon, is characterized by a high level of initial moisture after washing. Optimum drying of human hairs has an important role in final hair texture, homogeneity and flexibility. It is, therefore, required on general note to design dryers that are based on sub-Sahara Africa women's parameters. The understanding of the underline principles would usher in the development of indigenous hair dryer's technology for sub-Sahara Africans.

Therefore, this paper presents a mathematical model for the understanding of hair drying processes. Specifically, the model is developed for drying processes of women hair in saloons. The modelling is anchored on the conduction-convection heat transfer process, which culminates to the description of the physics of the drying processes; with appropriate boundary conditions being considered. The mathematics of the physics was solved using the method of separation of variable, as it presents itself as the appropriate solution method. The model is able to predict temperature and moisture content distributions of the drying hair; no available experimental data for comparison. However, the trend of results compared well with those of particular case of lump models. Simulations based on this model were conducted to study the effects of operational parameters (namely, air temperature, heat and mass transfer coefficients and mass and thermal diffusivities) on the moisture content and temperature of the hair. Simulation results show that increasing the air temperature and velocity decrease drying rate. It is evident from the simulations that sample with high thermal diffusivity and coefficient of diffusion values exhibits shorter duration of drying and that as the length of the hair increases from the origin (scalp), the temperature of the hair also increase, which means that temperature is highest at the tip of the hair.

The simulation results illustrated that the tip of the hair has the highest simulation temperature of 57.55^{0}C and the hair was completely dried up to 0.192kg/kg db moisture content when the dryer has worked for 48minutes. This further elaborates the efficiency of the developed models and conforms to the figures and literatures earlier cited. However, comparing the model with Dyson supersonic^{TM} hair dryer of 1600W, the estimated average efficiency of the model was calculated to be 70%. Further investigation showed that energy utilized by Dyson supersonic^{TM} hair dryer is higher as compared to the model; it implies that the higher amount of energy used by Dyson supersonic^{TM} hair dryer leads to faster drying rate and higher efficiency (100%). The lower amount of energy used by the model was to conserve energy and efficient in its task within the stipulated time.

REFERENCES

Afolabi, T.J. and Agarry, S.E.(2014). Mathematical modelling and simulation of the mass and heat transfer of batch convective air drying of tropical fruits. Chemical and Engineering Research, 23, 2224-7467.

Ayensu, A. (2003-2004). Thermal convection and moisture-diffusion in thin-layer fixed bed solar drying: National Industry and Social Science Sector. Council of Scientific and Industrial Research (CSIR), 9(1-2,3-4). Accra: Ghana.

Barati, E. and Esfahani, J. A. (2011). Mathematical modelling of convective drying: lumped temperature and spatially distributed moisture in slab. Journal of Energy, 36(4), 2294-2301.

Basirat, T.H. and Hamdullahpur, F. (2007). Mathematical modeling of drying based on surface evaporation source term for coupled energy and mass transfer. International Journal of Energy Research, 31(15), 1455-1464.

Clarence, R.R. 2012. Chemical and physical behaviour of human hair (5thed.). New York, USA: Springer.

Crank, J.1992. The Mathematics of Diffusion. Oxford, UK: Clarendon Press.

Darvishi, H., Azadbakht, M., Rezaeiasl, A. and Farhang, A. (2013). Drying characteristics of sardine fish dried with microwave heating. Journal of the Saudi Society of Agricultural Sciences, 12, 121-127.

Datta, A.K. (2007). Porous media approaches to studying simultaneous heat and mass transfer in food processes II: Property data and representative results. Journal of food Engineering, 80(1), 96-110

Evin, D. (2011). Thin layer drying kinetics of gundelia tournefortii L. Food and Bio-products and Processing, 9(2), 323-332.

Faghri, A. et al. (2010). Advanced Heat and Mass Transfer. Columbia: Global Digital Press.

Guoqing, L., .Huan, L. et al. (2014). Characterization of thermal transport in one-dimensional solid materials. Journal of Visualized Experiments, 83, 51144

Haghi, A.K. and Rondot, D. (2004). Heat and mass transfer in leader drying process. Iranian Journal of Chemistry and Chemical Engineering, 23(1), 25-34.

Jamaledddine, T.J. and Ray M.B. (2010). Application of computational fluid dynamics for simulation of drying process. A review of drying technology, 28(2), 120-1541.

Jiji, L. M. (2009). Heat Conduction (3rd ed.). Verlag Berlin Heidelberg: Springer, Inc.

Kumar, C., Karim A. et al. (2012). Modelling of heat and mass transfer process during convective drying of fruit. In Proceedings of the I4th International Conference Computational Methods. Gold Coast, Australia, November 25-27.

Luikov, A.V. (1968). Analytical Heat Diffusion Theory; London: Academic Press, Inc. Ltd.

Methakhup, S., Chewchan, N. and Devahastin, S. (2004). Effects of drying methods and conditions on drying kinetics and quality of Indian gooseberry flake. Journal of Food Engineering, 38(6), 579-587.

Mills, A.F. (1995). Basic Heat and Mass Transfer. Massachusetts: Irwin.

Mujumdar, A.S. (2004). Research and development in drying: Recent trends and future Protects. Drying Technology, 22(1-2), 1-26.

Mujumdar, A.S. (2007). Handbook of Industrial Drying. (3rded.). Boca Raton: CRC Press.

Nastaj, J.F. and Witkiewicz, K. (2009). Mathematical modelling of primary and secondary vacuum freeze drying of random solids at microwave heating. International Journal of Heat and Mass Transfer, 52(21-22), 4796-4806.

Ozisik, M.N. (1993). Heat Conduction (2nd ed.); New York: John Wiley and Sons, Inc.

Prabhanjan, D., Ramaswamy, H. and Raghavan, G. (1995). Microwave-assisted convective air drying of thin layer carrots: Journal of Food Engineering, (25), 283-293.

Quiroz, M.R.. and Nebra, S.A. (2001). Theoretical and experimental analysis of drying kinetics of banana. Journal of Food Engineering, 47(2), 127-132.

Simal, A., Femenia, A. et al. (2005). Use of exponential, pages and diffusion models to simulate the drying kinetics of kiwi fruit: Journal of food Engineering, 66(3), 323-328.

Srisittipokakun, N., Kirdsiri, K. and Kaekwkho, J. (2012). Solar drying of andrographis paniculata using parabolic shaped solar tunnel dryer. Journal of Procedia Engineering, 32, 839-846.

Worthman, F.J., Worthman, G. et al. (2010). Modulated differential scanning calorimetry of Human Hair in the Dry and Wet State. In Proceedings of the 10th European Symposium on Thermal Analysis and Calorimetry, Rotterdam, Netherlands, August 22-27.

Zhang, G., Wortmann, G. et al. (2011). Structure changes in human hair through bleaching as shown by Differential Scanning Calorimetry and Scanning Electron Microscopy. In Proceedings of the 17th International Hair-Science Symposium, Aachen, Germany, September 06-08